Graphene-Based Transparent Fabry-Perot Antenna in D-Band

M. U. Riaz*†, F. Paonessa*, G. V. Bianco‡, G. Bruno‡, A. D'Orazio§, L. Matekovits*†, G. Virone*
*Consiglio Nazionale delle Ricerche, IEIIT, Turin, Italy, giuseppe.virone@cnr.it
†Politecnico di Torino, DET, Italy
‡Consiglio Nazionale delle Ricerche, NANOTEC, Bari, Italy
§Politecnico di Bari, Dipartimento di Ingegneria Elettrica e dell'Informazione, Bari, Italy

***Abstract*—The limited bandwidth and availability of the electromagnetic spectrum below 100 GHz have led researchers to explore higher frequencies to provide high data transmission rates. This in turn requires innovative antenna technologies. This paper investigates the possibility of using multi-layer graphene to manufacture fully transparent antennas; i.e., antennas that can be integrated on a device screen. Experimental results in the D-band (110-170 GHz) show enhanced reflection behavior with respect to the glass support. This phenomenon is applied in constructing a transparent Fabry-Perot antenna. Simulated and measured results show good agreement, confirming the proposed design.**

***Index Terms*—Graphene, Fabry-Perot Antennas, SubTHz, Waveguide, Transparent Antennas.**

I. Introduction

There has been an immense growth in the generation and consumption of high-speed data from sources such as the internet. This surge in data requires next-generation wireless technologies to offer large bandwidth, unprecedented throughput and low latency [1] [2]. To meet these challenges, scientists and antenna researchers have shifted their focus towards high-frequency bands, such as subTHz. The subTHz band, spanning 100-300 GHz, offers large bandwidth to achieve high capacity [3][4]. However, this large bandwidth at these high frequencies is limited by low propagation distance due to both free-space and absorption losses [5].

A directive antenna system is required to improve the performance of the sub-THz link. This has led scientists to explore novel materials to achieve performance breakthroughs [6]. The transparency of the graphene and its high conductivity make it attractive to develop compact antennas that can be hidden in the screen of portable devices.

Reference [7] showed experimental results on a monolayer graphene in the sub-Thz range. In [6], multi-layer graphene has been characterized in X-band. In this work, we provide experimental results of doped and undoped multilayer graphene samples in the 110-170 GHz frequency range as a function of the number of layers. On the basis of the achieved material properties, we present the application of graphene in constructing a transparent Fabry-Perot antenna in the D-band (110-170 GHz). To the best of the authors' knowledge, this antenna solution is completely novel.

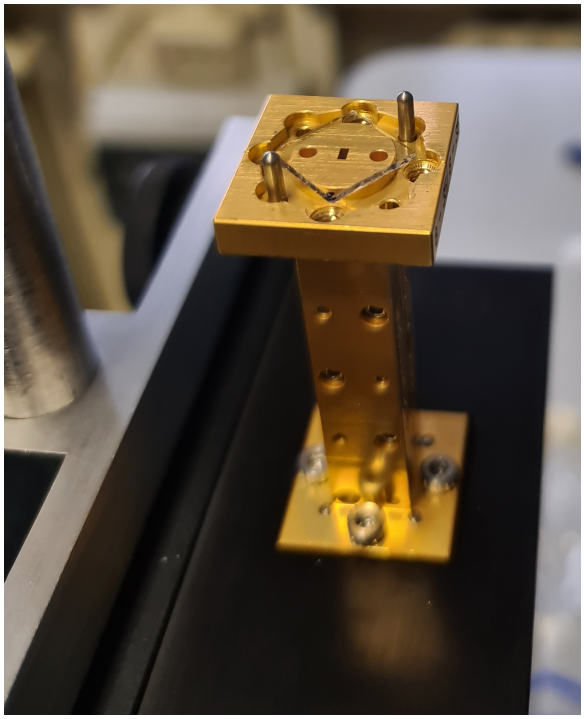

Fig. 1. Waveguide-based experimental setup in the 110-170 GHz frequency band.

II. Sample Characterization

Prior research has demonstrated that reconfigurable absorbers [6] and screens [8] can be obtained in the X band (7-13 GHz) by incorporating properly-engineered graphene layers. This concept has stimulated the characterization of such advanced material in the sub-THz band. With this aim, we conducted a series of experiments using multilayer graphene samples placed on top of an open-ended rectangular waveguide. Fig. 1 shows a straight section of WR6 (1.6 mm × 0.8 mm) metal waveguide connected to the millimeter-wave extender of a Vector Network Analyzer. A square-shaped graphene-coated glass sample (edge length 9 mm) is placed on top of such open-ended waveguide aperture. A set of such samples has been manufactured by CNR NANOTEC varying the number of graphene layers and doping. The samples were prepared using chemical vapour deposition (CVD) grown

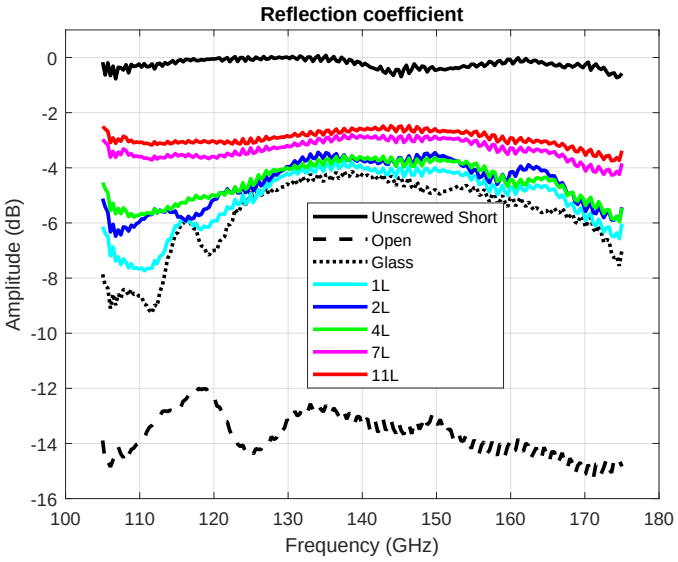

Fig. 2. Measured results of non-doped graphene samples in the 110-170 GHz frequency band.

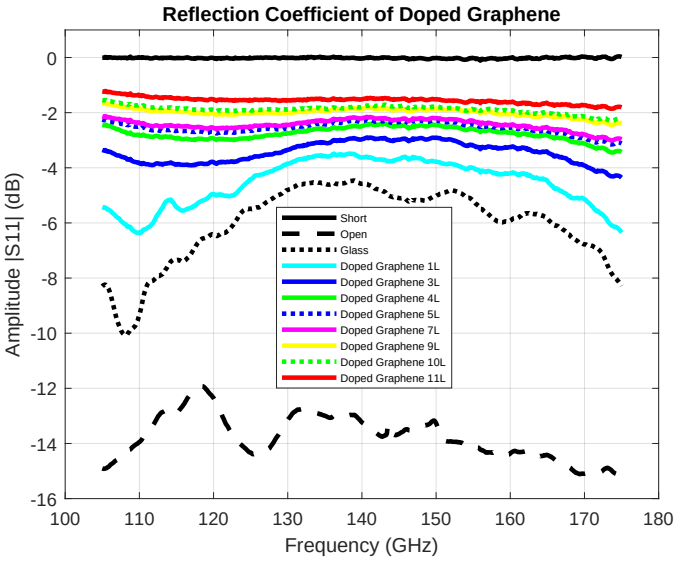

Fig. 3. Measured results of doped graphene samples in the 110-170 GHz frequency band.

graphene. In the measurement configuration of Fig. 1, the graphene layers (not visible due to transparency) are placed on the bottom of the sample i.e. in contact with the waveguide aperture. This setup operates as a waveguide short-circuit. The electromagnetic field is excited through the waveguide aperture, and the reflection coefficient is measured after proper calibration.

Fig. 2 and Fig. 3 present the experimental results obtained in the frequency range 110-170 GHz for non-doped and $SOCl_2$-doped graphene samples [9], respectively. As the number of graphene layers increases, a significant improvement of the reflection coefficient is observed. The doping of graphene is performed to increase the conductivity [8]. Therefore, doping also improves the reflection coefficient of the graphene-coated samples. The achieved reflection coefficients are far from the 0 dB of a metal conductor. This happens because the extracted conductivity of the graphene (not reported here for the sake of brevity) is lower than the metal one. Moreover, the thickness of a graphene layer is in the order of 0.34 nm, which is significantly smaller than the skin depth at this frequency (about 200 nm). Nevertheless, a significant improvement of reflectivity is visible with respect to the reference glass-only sample (black solid curve). Such phenomenon has been exploited to design and realize the transparent Fabry-Perot antenna discussed in the next section.

III. Fabry-Perot Antenna

The experimental measurements of composite layers of glass and graphene behave as a partially reflective surface (PRS). Such a PRS has been used to design a transparent Fabry-Perot (FP) antenna. The FP antenna, also known as a 2D leaky wave antenna [10], operates on the principle of constructive interference of standing waves that occur inside the FP cavity [11]. A FP antenna is formed by placing the PRS at approximately $\lambda/2$ from the fully reflective metal flange of the WR6 waveguide, as sketched in Fig. 4. When the electromagnetic field is excited by the radiator (open-ended waveguide), part of the wave is transmitted through the PRS while the remaining part is repeatedly reflected between the two surfaces. The reflectivity of PRS can be controlled by the number of graphene layers. Thus, the directivity of FP antenna can be controlled by selecting the number of graphene layers.

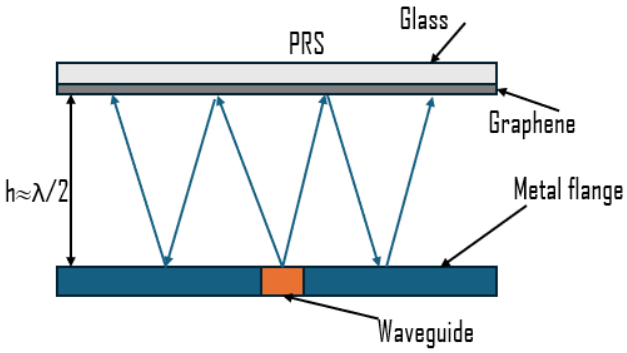

Fig. 4. Conceptual model of FP antenna.

IV. Experimental Results

A graphene-based transparent FP antenna has been designed to operate at a central frequency of 140 GHz. The composite layers of glass (0.7mm) and ll layers of doped graphene (approximately 4nm) have been used as PRS. Dielectric spacers were fabricated to maintain the PRS at a distance of 1.07mm from the waveguide metal flange. This configuration was modelled in CST software [12]. The assembled prototype was measured in farfield setup.

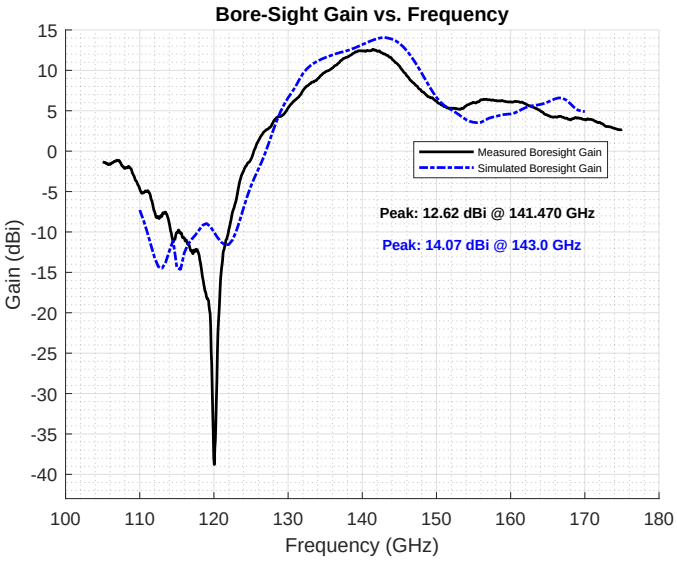

Fig. 5. FP antenna boresight gain.

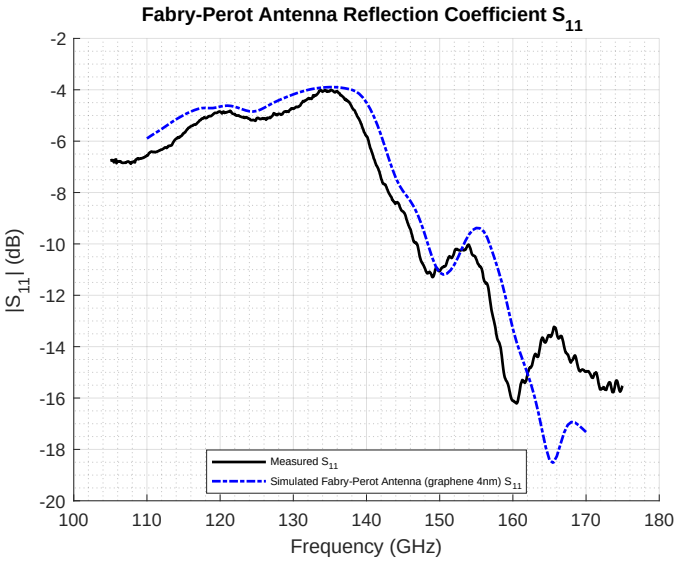

Fig. 6. FP antenna reflection coefficient.

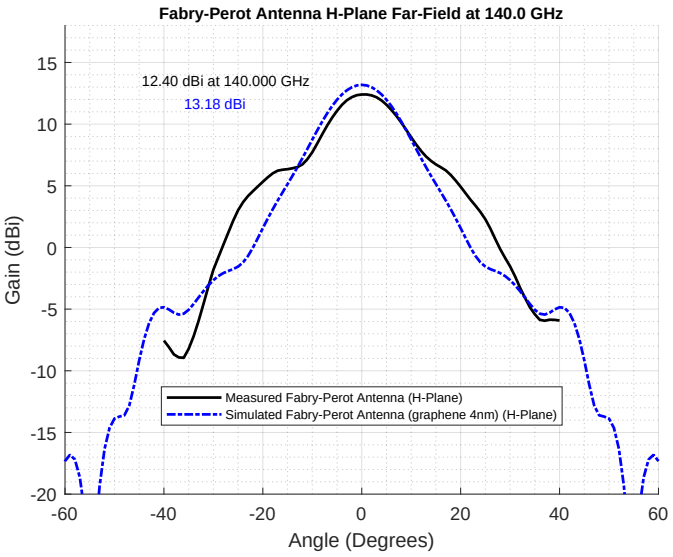

Fig. 7. Antenna H plane farfield at 140 GHz.

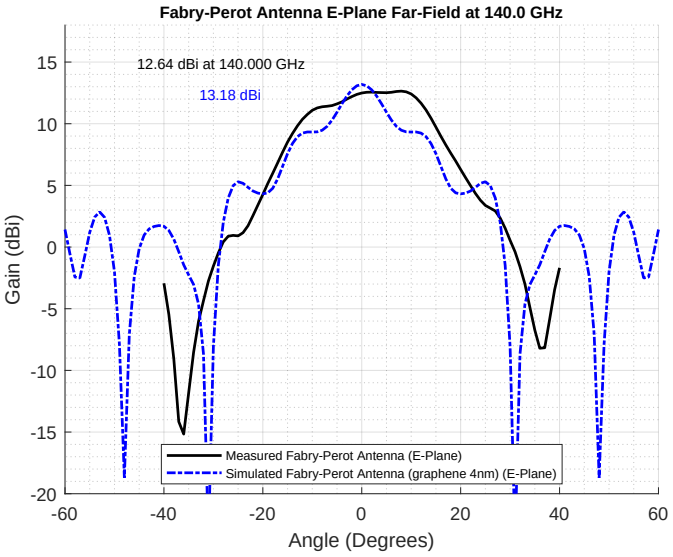

Fig. 8. Antenna E plane farfield at 140 GHz.

Fig. 5 presents the measured and simulated boresight gain. It is apparent that the antenna resonates at 140 GHz with a maximum gain of about 12 dBi, which is an improvement with respect to an open-ended waveguide (about 7 dBi). Fig. 6 shows the reflection coefficient results, in the frequency range of 110-170 GHz. The simulated and measured results are in good agreement. The reflection level at 140 GHz is only -6 dB because the present prototype did not include any matching elements. This feature will be considered in future developments. Fig. 7 and Fig. 8 show the measured and simulated results for the H- and E- planes, respectively. A sufficient agreement has been achieved. The discrepancies are mainly due the small thickness of graphene (about 4nm) compared to wavelength which caused significant convergence and accuracy problems in CST software. As already mentioned above, the graphene thickness is also smaller than the skin depth. Therefore, such material was modelled as a penetrable dielectric (and not as a lossy conductor) with a very small thickness with respect to the mesh size.

V. Conclusion

This paper presented the experimental results of doped and undoped multilayer graphene samples obtained in the frequency range of 110-170 GHz. The number of layers affects the reflection coefficient of such a composite partially reflective surface. This phenomenon has been used to design a transparent Fabry-Perot antenna operating at 140 GHz. The measured data show good agreement with the simulated data.

Future work will deal with the design of a matching element in WR6 waveguide and the exploration of reconfigurable

properties of graphene. We opted to build the FP antenna on top of the WR6 flange to allow seamless integration with the measurement setup (similar to Fig. 1). Future versions will include different coupling strategies, e.g. ground plane slots.

ACKNOWLEDGMENT

The antenna design has been partially supported by the European Union under the Italian National Recovery and Resilience Plan (NRRP) of NextGenerationEU, partnership on "Telecommunications of the Future" (PE00000001 – program "RESTART"). The measurement setup and the data analysis have been partially developed in the framework of SoBigData.it (Smart Radio Environment). SoBigData.it receives funding from European Union —NextGenerationEU-National Recovery and Resilience Plan (Piano Nazionale di Ripresa e Resilienza, PNRR) —Project: "SoBigData.it —Strengthening the Italian RI for Social Mining and Big Data Analytics" — Prot. IR0000013 —Avviso n. 3264 del 28/12/2021.

REFERENCES

[1] T. S. Rappaport et al., "Wireless Communications and Applications Above 100 GHz: Opportunities and Challenges for 6G and Beyond," in IEEE Access, vol. 7, pp. 78729-78757, 2019, doi: 10.1109/ACCESS.2019.2921522.

[2] S. Thomas, J. Singh Virdi, A. Babakhani and I. P. Roberts, "A Survey on Advancements in THz Technology for 6G: Systems, Circuits, Antennas, and Experiments," in IEEE Open Journal of the Communications Society, vol. 6, pp. 1998-2016, 2025, doi: 10.1109/OJCOMS.2025.3549710.

[3] Y. He, Y. Chen, L. Zhang, S. -W. Wong and Z. N. Chen, "An overview of terahertz antennas," in China Communications, vol. 17, no. 7, pp. 124-165, July 2020, doi: 10.23919/J.CC.2020.07.011.

[4] I. Atzeni et al., "Sub-THz Communications: Perspective and Results From the Hexa-X-II Project," in IEEE Open Journal of the Communications Society, vol. 6, pp. 7495-7540, 2025, doi: 10.1109/OJCOMS.2025.3591836.

[5] Pant R, Malviya L. THz antennas design, developments, challenges, and applications: A review. Int J Commun Syst. 2023; 36(8):e5474. doi:10.1002/dac.5474.

[6] Grande, M., Bianco, G.V., Perna, F.M. et al., Reconfigurable and optically transparent microwave absorbers based on deep eutectic solvent-gated graphene. Sci Rep 9, 5463 (2019). https://doi.org/10.1038/s41598-019-41806-w

[7] Dadrasnia, E., Puthukodan, S., Thalakkatukalathil, V.V., Lamela, H., Ducournau, G., Lampin, J.F., Garet, F. and Coutaz, J.L., 2014. Sub-THz Characterisation of Monolayer Graphene. Journal of Spectroscopy, 2014(1), p.601059.

[8] M. Grande, G. V. Bianco, M. A. Vincenti, D. de Ceglia, P. Capezzuto, V. Petruzzelli, M. Scalora, G. Bruno, and A. D'Orazio, Optically transparent microwave screens based on engineered graphene layers, Opt. Express 24, 22788-22795 (2016)

[9] Bianco, G.V., Sacchetti, A., Milella, A., Grande, M., D'Orazio, A., Capezzuto, P. and Bruno, G., 2020. Extraordinary low sheet resistance of CVD graphene by thionyl chloride chemical doping. Carbon, 170, pp.75-84.

[10] J. R. Kelly, T. Kokkinos and A. P. Feresidis, "Analysis and Design of Sub-Wavelength Resonant Cavity Type 2-D Leaky-Wave Antennas," in IEEE Transactions on Antennas and Propagation, vol. 56, no. 9, pp. 2817-2825, Sept. 2008, doi: 10.1109/TAP.2008.928791.

[11] L. Zhiming, B. Jens, L. Shaobin and K. Xiangkun, "Investigations and prospects of Fabry-Perot antennas: A review," in Journal of Systems Engineering and Electronics, vol. 32, no. 4, pp. 731-747, Aug. 2021, doi: 10.23919/JSEE.2021.000063.

[12] https://www.3ds.com/products/simulia/cst-studio-suite